SRTTU

JCARME
ISSN: 2228-7922
Journal of Computational and Applied Research in Mechanical Engineering
Vol. 10, No. 1, pp. 37-49
jcarme.sru.ac.ir

Entropy generation analysis of MHD forced convective flow through a horizontal porous channel

Tarun Sharma[a], Pooja Sharma[a,*] and Navin Kumar[b]

[a]*Department of Mathematics and Statistics, Manipal University Jaipur, Jaipur, Rajasthan, 303007, India*
[b]*Department of Mathematics, Indian Military Academy, Dehradun, Uttarakhand,24800, India*

Article info:

Type:	Research
Received:	01/04/2019
Revised:	22/08/2019
Accepted:	25/08/2019
Online:	25/08/2019

Keywords:
MHD,
Forced convection,
Heat source,
Inclined magneitc field,
Entropy generation.

Abstract

Entropy generation due to viscous incompressible MHD forced convective dissipative fluid flow through a horizontal channel of finite depth in the existence of an inclined magnetic field and heat source effect has been examined. The governing non-linear partial differential equations for momentum, energy, and entropy generation are derived and solved by using the analytical method. In addition, the skin friction coefficient and Nusselt number are calculated numerically and their values are presented through the tables for the upper and the bottom wall of the channel. It was concluded that the total entropy generation rate and Bejan number are reduced due to a rise in the inclination angle of the magnetic field. Also, an increment in the heat source props up the fluid temperature and total entropy generation rate. This study will help to reduce the energy loss due to reversible process and heat dissipation. The results are also useful for chemical and metallurgy industries.

1. Introduction

Magnetohydrodynamic flow has a notable interest in diverse fields of industries and engineering. Agriculture industries, groundwater hydrology, filtration and separation process in the chemical and petroleum industries, metallurgy, oceanography, plasma physics, designing of cooling devices, cooling of nuclear and power plant, cooling of electronic devices, MHD power generator, etc. are various applications in science and technology. In the last few decades, it is found that MHD flow has dominated the industries due to its wide use and dependency in every field of science and technology. Hannes Alfven, a plasma physicist was the first scientist who used the term MHD and for it, he received a prestigious Nobel Prize in physics in year 1970. The MHD flow through different geometries has been widely studied in the last half-century. In the literature, we found that Raptis [1] contributed to the two-dimensional natural convective flow through the porous medium. Vanka et al. [2] investigated the three-dimensional magnetohydrodynamic fluid flow in the channel. In the continuation, Ghosh et al. [3] inspected the hydromagnetic fluid flow in a rotating system. Krishna et al. [4] discussed the MHD convective fluid flow in a rotating channel due to the heat source effect. An analytical study for MHD natural convective flow through the vertical channel has been

[*]*Corresponding author*
email address: pooja_2383@yahoo.co.in

discussed by Singh [5] using the perturbation method. In their study, they found that a rise in the magnetic field and permeability reduces the fluid velocity.

Mhone et al. [6] surveyed the MHD flow through the diverging channel in the existence of an applied transverse magnetic field. In this study, it is seen that the high strength of the applied magnetic field slows down the motion of the fluid. MHD couette flow in the rotating channel under the influence of the magnetic field was reported by Seth et al. [7]. It is viewed that the amplification in the strength of the magnetic field reduces the fluid motion, whereas the effect of inclination angle reflects adversely. Later, Seth et al. [8] expanded their previous work and discussed the Hall Effect in a rotating system. The effect of the inclined magnetic field in MHD poiseuille flow through the two-plate channel was explained by Manyonge et al. [9] and validated the results discussed by other researchers for magnetic field and velocity profile. Later, Joseph et al. [10] examined the impact of the inclined magnetic field in MHD couette flow through parallel plate channel. They noticed that the velocity of fluid and coefficient of skin friction diminish with the increment in the stability of the inclined magnetic field parameter. Raju et al. [11] explored the MHD forced convective flow through the horizontal porous channel in the existence of the viscous dissipation effect. It is seen that fluid velocity enhanced with the rise in the permeability parameter, while the opposite effect is observed for improving the strength of the magnetic field. Later, MHD fluid flow between two horizontal plates has been studied by Mburu et al. [12]. In this analysis, it is noticed that the pressure gradient helps the rising of the fluid motion. Sharma et al. [13] analyzed the MHD flow in a horizontal porous channel with chemical reaction, thermal radiation and heat source effect.

Entropy generation minimization is the concept of reducing thermodynamic irreversibility. In thermal, chemical and petroleum industries, there are many factors that produce the entropy in the system during the fluid flow, such as a change in the temperature difference, viscous dissipation, and friction due to fluid particles during the motion. Sometimes applied external magnetic field also plays the main reason of irreversibility in the system. In the thermal industries and engineering domain, the main aim of the scientist is to attain the maximum efficiency with minimum energy loss. For optimizing the thermodynamic efficiency, researchers and scientists design and develop such thermal systems that provide high efficiency with minimum irreversibility. The pioneer and remarkable study on entropy generation minimization are done by Bejan [14, 15]. Irreversibility distribution due to MHD natural convective flow through a cavity was scrutinized by Mahmud et al. [16]. Later, Mahmud et al. [17] expanded the previous work and examined the entropy generation in the horizontal porous channel due to viscous dissipation. Total irreversibility distributions in terms of entropy generation profiles in a horizontal channel were investigated by Damesh et al. [18] by taking the applied magnetic field and viscous dissipation into account. In this study, they found that entropy generation rate is decayed when the strength of the magnetic field props up. Bouabid et al. [19] inspected the entropy generation in the square porous cavity due to the inclined magnetic field and thermosolutal convection. A study of entropy generation due to the effect of a suction/injection and navier slip was explored by Eegunjobi and Makinde [20]. In the same year, Eegunjobi and Makinde [21] extended the previous work to investigate the entropy generation through a vertical porous channel due to the navier slip and buoyancy force effect. In the continuation, Makinde and Eegunjobi [22] investigated the irreversibility for variable viscosity and magnetic field effect through a horizontal channel. In this study, they found that boost in the transverse magnetic field decelerates the fluid motion, whereas an increase in the strength of magnetic field props up the fluid temperature. Further, entropy generation due to heat transfer in water-based nanofluid through the horizontal open cavity was deliberated by Mehrez et al. [23]. Later, Adesanya and Makinde [24, 25] explored the irreversibility due to a couple stress effect through a porous channel by using the analytical technique. Meanwhile, Makinde and

Eegunjobi [26] investigated the irreversibility distribution due to casson fluid flow in a microchannel in the existence of an applied magnetic field and radiation effect. In the continuation, total irreversibility distribution in a horizontal circular channel was investigated by Sharma et al. [27] by considering the viscous dissipation, transverse magnetic field, and radiation effect. They analyzed the effect of diverse fluid flow parameters on the entropy generation profile and provided the key parameter that regulates the irreversibility for fluid flowing through circular systems.

In the same ideology, for filling the gap in the literature, we are inspired by the discussed works and investigated the entropy generation due to magnetohydrodynamic, forced convective flow in a porous medium filled horizontal channel in the influence of the inclined magnetic field, viscous dissipation and heat source effect.

2. Mathematical formulation

A steady viscous incompressible electrically conducting forced convective fluid flow through a fixed horizontal channel filled with the porous medium under the influence of inclined magnetic field and heat source is considered. The upper surface of the channel is considered open for the environment with the constant temperature T_1^* whereas the bottom surface is taken thermally insulated and impermeable with the temperature T_0^*. For the geometry of the flow scheme, we have chosen a cartesian coordinate system with the origin O at the bottom surface having the depth H^* from the upper open surface.

The y^* coordinate system is taken along the depth of the channel and the x^* is taken along the fluid velocity u^*. The fluid flow is supposed to be possible due to the constant pressure gradient as shown in Fig. 1. It is considered that the Reynolds number for this inclined magnetic field is sufficiently small; therefore, the induced magnetic field is negligible.

Darcy law discussed by Yamamoto et al. [28] is considered in the momentum equations. Under these conditions, the system of equations for the present flow scheme is given below:

$$\frac{\partial u^*}{\partial x^*} = 0, \tag{1}$$

$$-\frac{\partial P^*}{\partial x^*} + \mu \frac{\partial^2 u^*}{\partial y^{*2}} - \mu \frac{u^*}{K^*} - \sigma B_0^2 \sin^2 \alpha \; u^* = 0, \tag{2}$$

$$\rho C_p u^* \frac{\partial T^*}{\partial x^*} = \kappa \frac{\partial^2 T^*}{\partial y^{*2}} + \mu \left(\frac{\partial u^*}{\partial y^*} \right)^2 + \sigma B_0^2 \sin^2 \alpha \; u^{*2} + Q^* \left(T^* - T_0^* \right), \tag{3}$$

The corresponding boundary conditions are given as:

$$y^* = 0 : u^* = 0, \frac{\partial T^*}{\partial y^*} = 0,$$

$$y^* = H^* : \mu \frac{\partial u^*}{\partial y^*} = 0, T^* = T_1^*, \tag{4}$$

where P^* is given for pressure, μ^* is denoted for the dynamic viscosity, K^* stands for the permeability parameter of the porous medium, σ is the electrical conductivity, B_0 is denoted for magnetic field, ρ stands for the fluid density, T^* shows the fluid temperature, H^* is the depth of the channel, κ represents the thermal conductivity, α is denoted for the inclination angle of magnetic field, Q^* for the heat source parameter and C_p is given for the specific heat at constant pressure.

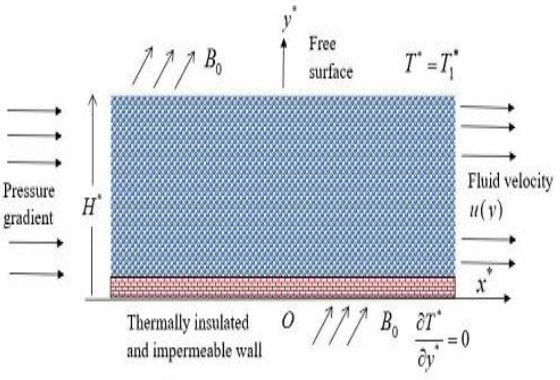

Fig. 1. Geometry configuration.

3. Method of solution

Introducing the following dimensionless quantities:

$$\frac{x^*}{h}=x,\quad \frac{y^*}{h}=y,\ \frac{H^*}{h}=h_1,\ u^*=\frac{\mu u}{\rho h},$$
$$P^*=\frac{\mu^2 P}{\rho h^2},\quad M=\frac{\sigma B_0^2 h^2}{\mu},\ P_2=\frac{\partial T}{\partial x},\ K^*=\frac{h^2}{K^2},$$
$$\frac{\partial P^*}{\partial x^*}=\frac{\mu^2}{\rho h^3}P_1\left(P_1=-\frac{\partial P}{\partial x}\right),\ \mathrm{Pr}=\frac{\mu C_p}{\kappa},$$
$$Q^*=\frac{Q\kappa}{h^2},\quad M_1=\left(K^2+M\sin^2\alpha\right),$$
$$T=\frac{T^*-T_0^*}{T_1^*-T_0^*},\qquad Br=\frac{\mu^3}{\rho^2 h^2\kappa\left(T_1^*-T_0^*\right)},\qquad (5)$$

into the governing Eqs. (2) and (3), then:

$$\frac{d^2u}{dy^2}-M_1u=-P_1,\qquad (6)$$

$$\frac{d^2T}{dy^2}+QT=-Br\left(\frac{du}{dy}\right)^2-M\sin^2\alpha\,Br\,u^2+\mathrm{Pr}\,P_2\,u,\qquad (7)$$

The dimensionless boundary conditions are given as:

$$y=0:\ u=0,\ \frac{\partial T}{\partial y}=0,$$
$$y=h_1:\ \frac{\partial u}{\partial y}=0,\quad T=1,\qquad (8)$$

Now, the complete solutions of the Eq. (6) and Eq. (7) are obtained under the defined boundary condition (8) by the usual algebraic method and presented as below:

$$u(y)=B_2e^{\sqrt{M_1}y}+B_3e^{-\sqrt{M_1}y}+\frac{P_1}{M_1},\qquad (9)$$

$$T(y)=B_{30}\cos\left(\sqrt{Q}\right)y+B_{27}\sin\left(\sqrt{Q}\right)y+B_{22}e^{2\sqrt{M_1}y}+B_{23}e^{-2\sqrt{M_1}y}+B_{24}+B_{25}e^{\sqrt{M_1}y}+B_{26}e^{-\sqrt{M_1}y}.\qquad (10)$$

Here B_2 to B_{30} and M_1 are constants. These constants are not presented here for the sake of brevity.

4. Skin friction coefficient

The coefficient of skin friction C_{f_0} and C_{f_1} at the insulated bottom wall and upper surface of the channel is calculated respectively, and their expression is given as:

$$C_{f_0}=\frac{\tau_w}{\left(\frac{\rho u^2}{2}\right)}=\frac{\mu}{\left(\frac{\rho u^2}{2}\right)}\left(\frac{\partial u^*}{\partial y^*}\right)_{y^*=0}=\frac{2}{\mathrm{Re}^2}\left(\frac{\partial u}{\partial y}\right)_{y=0},\qquad (11)$$

$$C_{f_1}=\frac{\tau_w}{\left(\frac{\rho u^2}{2}\right)}=\frac{\mu}{\left(\frac{\rho u^2}{2}\right)}\left(\frac{\partial u^*}{\partial y^*}\right)_{y=H^*}=\frac{2}{\mathrm{Re}^2}\left(\frac{\partial u}{\partial y}\right)_{y=h_1},\qquad (12)$$

5. Nusselt number

The heat transfer coefficient in terms of the Nusselt number Nu_0 and Nu_1 at the insulated bottom wall and upper surface of the channel is calculated respectively, and their expression is given as:

$$Nu_0=\left(\frac{dq_{(x)}}{\kappa\left(T_1^*-T_0^*\right)}\right)=-\frac{h\kappa}{\kappa\left(T_1^*-T_0^*\right)}\left(\frac{\partial T^*}{\partial y^*}\right)_{y^*=0},$$
$$Nu_0=-\left(\frac{\partial T}{\partial y}\right)_{y=0},\qquad (13)$$

$$Nu_1=\left(\frac{dq_{(x)}}{\kappa\left(T_1^*-T_0^*\right)}\right)=-\frac{h\kappa}{\kappa\left(T_1^*-T_0^*\right)}\left(\frac{\partial T^*}{\partial y^*}\right)_{y^*=H^*},$$
$$Nu_1=-\left(\frac{\partial T}{\partial y}\right)_{y=h_1},\qquad (14)$$

6. Entropy generation

Analytical study of total entropy generation due to MHD forced convective fluid flow in a porous medium filled horizontal channel under the existence of inclined magnetic field and heat source is considered for minimizing the total irreversibility distribution in terms of entropy generation rate. Entropy generation is caused due to fluid friction, viscous dissipation and the most important due to the magnetic field. In the engineering and industrial field, it is necessary to

obtain the high efficiency and optimal design of all devices that work on the basis of the second law of thermodynamics. According to Wood [29] and Bejan [14, 30], the entropy generation is specified as:

$$S_{gen}''' = \frac{\kappa}{\left(T_0^*\right)^2}\left(\frac{\partial T^*}{\partial y^*}\right)^2 + \frac{\mu}{\left(T_0^*\right)}\left[\left(\frac{\partial u^*}{\partial y^*}\right)^2 + \frac{u^{*2}}{K^*}\right] + \frac{\sigma B_0^2}{\left(T_0^*\right)}\sin^2\alpha\left(u^*\right)^2, \quad (15)$$

Now, using the dimensionless quantities defined in the Eq. (5) into the Eq. (15), the entropy generation parameter in non-dimensional form is found as:

$$Ns = \frac{S_{gen}'''}{S_0'''} = \left(\frac{dT}{dy}\right)^2 + Br\,T_0\left\{\left(\frac{du}{dy}\right)^2 + K^2u^2\right\} + Br\,M\,T_0\sin^2\alpha\,u^2 \quad (16)$$

Here the first, second, and third terms of the Eq. (16) represent the irreversibility due to the heat transfer, fluid friction, viscous dissipation, and inclined magnetic field, respectively.

where $T_0 = \frac{T_0}{\left(T_1^* - T_0^*\right)}$ is the reference temperature in the dimensionless form and $S_0''' = \frac{\kappa}{T_0^2 h^2}$ defines the reference volumetric entropy generation.

The Bejan number Be is also calculated. It is the ratio of irreversibility due to heat transfer $\left(Ns_1\right)$ and total irreversibility $\left(Ns\right)$ and expressed as:

$$Be = \frac{Ns_1}{Ns}, \quad (17)$$

where irreversibility is measured in terms of entropy generation rate.

The characteristic value of the Bejan number lies between 0 and 1. The Bejan number $Be = 1$ shows that irreversibility due to more impact of heat transfer and the reverse effect is seen in the case of $Be = 0$. Although $Be = 0.5$ defines that the irreversibility due to an equal contribution of heat transfer to the viscous dissipation, fluid friction, and magnetic field.

7. Results and discussion

The analysis of the present flow scheme is very helpful for understanding many natural and artificial flows in nature and industries. In the present paper, an analytical solution is obtained and discussed through figures for fluid velocity and temperature profile by using the MATLAB software. Later, the irreversibility parameters in terms of entropy generation rate as well as Bejan number are also investigated for the same flow configuration with various physical parameters.

7.1. Velocity profile

The physical importance of various flow parameters has been shown for the velocity distribution profile from Fig. 2 to Fig. 4. Fig. 2 describes the effect of pressure gradient P_1, permeability parameter K and applied inclined magnetic field M on the fluid velocity by keeping $\alpha = \pi/4$ and the depth of the channel $h_1 = 1.0$. It is seen that the fluid velocity is raised with the growth in the pressure gradient; whereas an increment in the permeability parameter and an inclined magnetic field parameter decline the fluid velocity. It is obvious that the fluid always reduces its motion when the magnetic field is strong. Further, Fig. 3 shows the effect of the inclination angle α of the magnetic field with the velocity distribution of fluid by keeping the other parameters fixed. The fluid velocity is decreasing with a rise in the value of α from $\alpha = 0$ to $\alpha = \pi/2$. The fluid velocity is boosted with the rise in the depth of the channel as observed from Fig. 4. It is due to the fact that the fluids flowing through a higher depth of the channel have less resistance with the comparison to a channel of the small depth.

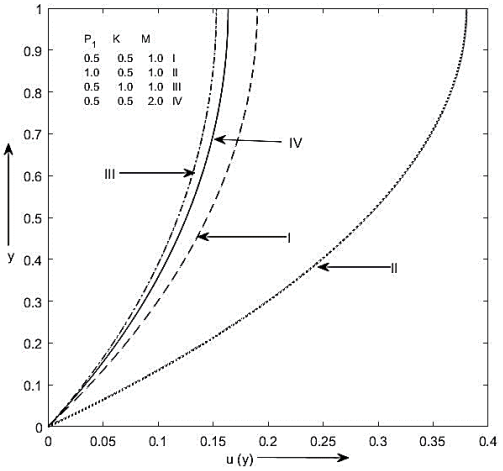

Fig. 2. Velocity profile versus y, when $\alpha = \frac{\pi}{4}$, $h_1 = 1.0$.

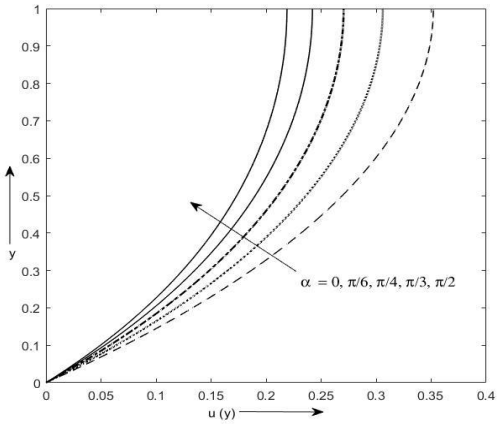

Fig. 3. Velocity profile versus y, when $M = 2.0, P_1 = 1.0, K = 1.0, h_1 = 1.0$.

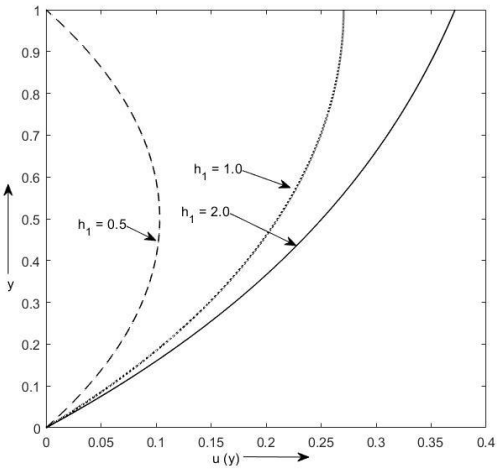

Fig. 4. Velocity profile versus y, when $M = 2.0, P_1 = 1.0, K = 1.0, \alpha = \frac{\pi}{4}$.

7.2. Temperature profile

The effect of physical parameters for temperature distribution profiles have been displayed from Fig. 5 to Fig. 8. It is observed from Fig. 5 that the high intensity of inclined magnetic field M and the permeability K decrease the temperature distribution in the channel for the fixed value of α i.e., at $\alpha = \pi/4$ whereas the growth in the Prandtl number $\Pr = 0.005$ (liquid sodium) to $\Pr = 7.0$ (water) enhances the temperature distribution of fluid throughout the channel. In a nuclear reactor or power plant, liquid sodium is used as a coolant for regulating the temperature. It is depicted from Fig. 6 that an increment in the α from $\alpha = 0$ to $\alpha = \pi/2$ decay the fluid temperature. Fig. 7 explains that the fluid temperature upsurges with an increment in the depth of the channel. Fig. 8 shows that a rise in the pressure gradient helps to reduce the fluid temperature, whereas gain in the heat source reflects the adverse behavior. It is a fact that the heat source always works as some extra heat to the fluid, and due to this reason; the fluid temperature boosts in the channel. Fig. 8 also explains that the growth in the Brinkmann number helps to create the internal resistance during the fluid motion, and therefore it promotes the gain in the fluid temperature.

7.3. Entropy generation profile

In thermal industries, the total entropy generation in the process should be minimum for obtaining the ideal and optimized state of the devices. In order to achieve the thermodynamic efficiency, the entropy generation in the present flow scheme has been discussed from Fig. 9 to Fig. 13. Fig. 9 defines the influence of the inclined magnetic field M and permeability K with the irreversibility parameter Ns with the fixed channel depth $h_1 = 1.0$ and the fixed inclination angle of the magnetic field $\alpha = \pi/4$. It is found that the improvement in the M and K helps to reduce the irreversibility parameter Ns in the flow scheme.

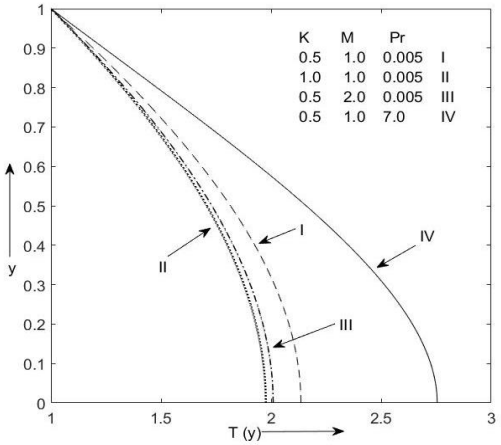

Fig. 5. Temperature profile versus y, when $h_1 = 1.0, P_1 = 1.0,\ P_2 = 1.0, Br = 0.5, Q = 1.0\ , \alpha = \frac{\pi}{4}$

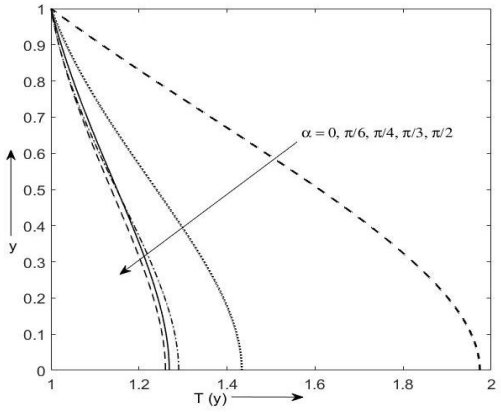

Fig. 6. Temperature profile versus y, when $h_1 = 1.0, P_1 = 1.0, P_2 = 1.0, Br = 0.5, Q = 1.0, M = 2.0, K = 1.0, Pr = 7.0$.

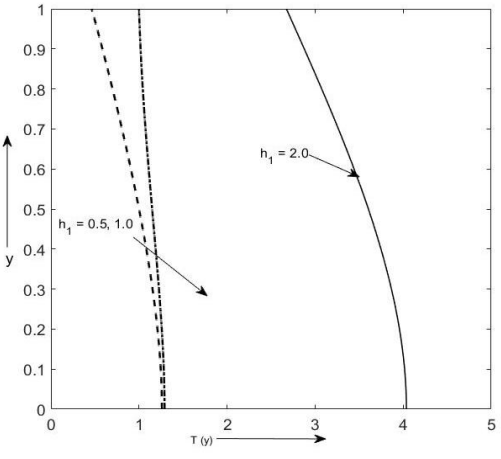

Fig. 7. Temperature profile versus y, when $\alpha = \frac{\pi}{4}, P_1 = 1.0, P_2 = 1.0,\ Br = 0.5,\ Q = 1.0\ , M = 2.0,\ K = 1.0, Pr = 7.0$.

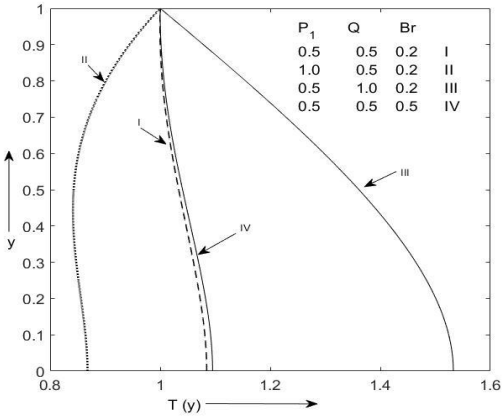

Fig. 8. Temperature profile versus y, when $\alpha = \frac{\pi}{4}, P_2 = 1.0, h_1 = 1.0, M = 2.0, K = 1.0, Pr = 7.0$.

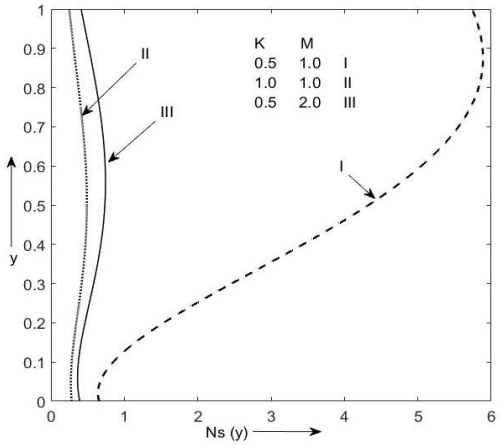

Fig. 9. Ns profile versus y, when $\alpha = \frac{\pi}{4}, P_2 = 1.0, h_1 = 1.0, P_1 = 1.0, Q = 1.0, Br = 0.5\ Pr = 7.0$.

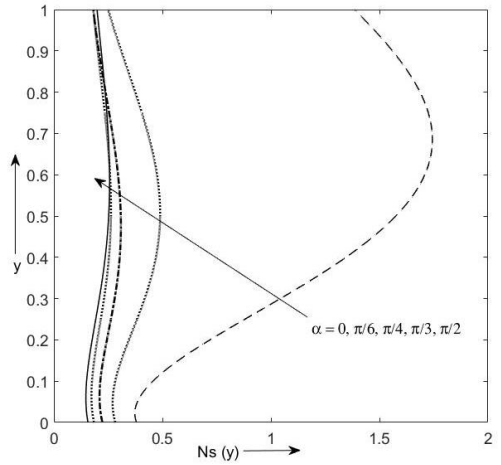

Fig. 10. Ns profile versus y, when $K = 1.0,\ M = 2.0\ P_2 = 1.0, h_1 = 1.0,\ P_1 = 1.0, Q = 1.0, Br = 0.5\ Pr = 7.0$.

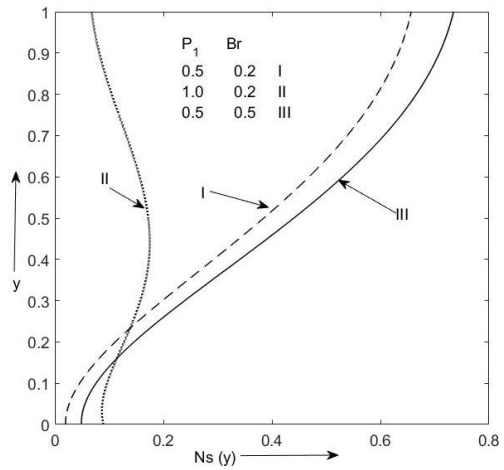

Fig. 11. Ns profile versus y, when $K = 1.0, M = 2.0\ P_2 = 1.0, h_1 = 1.0, \quad \alpha = \frac{\pi}{4}, Q = 1.0, Pr = 7.0.$

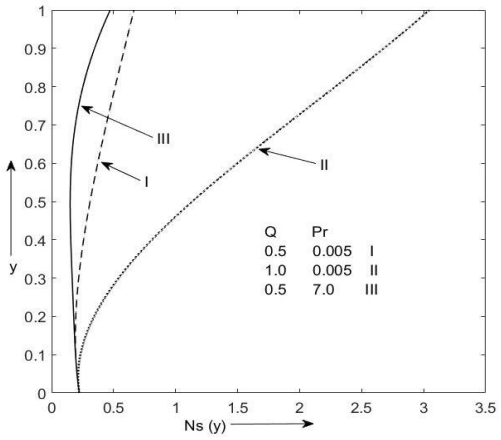

Fig. 12. Ns profile versus y, when $K = 1.0, M = 2.0\ P_2 = 1.0, h_1 = 1.0, \alpha = \frac{\pi}{4}, P_1 = 1.0, Br = 0.5.$

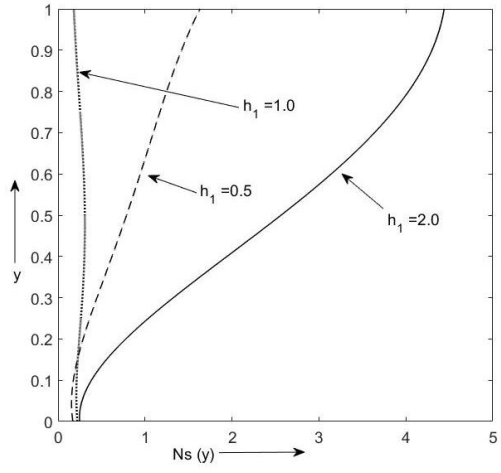

Fig. 13. Ns profile versus y, when $K = 1.0, M = 2.0\ P_2 = 1.0, Q = 1.0, \quad \alpha = \frac{\pi}{4}, P_1 = 1.0, Br = 0.5, Pr = 7.0.$

Fig. 10 depicts that the total irreversibility rate is decreased with an increment in the α form $\alpha = 0$ to $\alpha = \pi/2$.

Further, Fig. 11 shows that the irreversibility parameter in the channel is decreased with an increase in the pressure gradient P_1, whereas the opposite effect is seen with the rise in the Brinkmann number Br. It is physically valid; because of the increase in the strength of Brinkmann number Br enhances the fluid temperature, therefore the total irreversibility distribution parameter Ns upsurges in the channel. The impact of heat source parameter Q and Prandtl number Pr with entropy generation number Ns is portrayed from Fig. 12. It is visible that the irreversibility parameter Ns is increased with a rise in Q; it is due to the fact that an increase in the intensity of heat source Q boosts the fluid temperature, and therefore the total entropy generation increases; on the other hand, entropy generation in the channel is decayed when the value of Pr upsurges. In the present analysis, we have discussed two different types of fluid flow with entropy generation as $\mathrm{Pr} = 0.005$ is considered for liquid sodium and $\mathrm{Pr} = 7.0$ is the ideal value of water. It is the fact that liquid sodium helps to reduce the fluid temperature and works as a coolant in the nuclear reactor or power plant. The depth of the channel also helps to control the entropy generation in the channel as observed from Fig. 13. It is seen that entropy generation is increased with the rise in the depth of the channel.

7.4. Bejan number profile

The irreversibility ratio in terms of Bejan number Be is also discussed for different physical parameters from Fig. 14 to Fig. 18. The influence of the permeability K and the inclined magnetic field M on the Bejan number has been discussed in Fig. 14 with a fixed value of $\alpha = \pi/4$ and a fixed depth of the channel $h_1 = 1.0$. It is seen that the high intensity of the magnetic field M and the permeability K reduces the Bejan number Be. Further, Fig. 15 describes that an enhancement in the α form

$\alpha = 0$ to $\alpha = \pi/2$ declines the Bejan number Be , because of the fluid temperature decreases with an increased value of the angle, therefore the Bejan number decreases. Fig. 16 displays the impact of pressure gradient P_1 and Brinkmann number Br with irreversibility ratio Bejan number Be. It is noticed that an increment in the strength of the Brinkmann number Br and pressure gradient P_1 decrease the Bejan number. Further, Fig. 17 shows the influence of heat source Q and Pr with Bejan number Be. It is depicted that the rise in the heat source Q enhances the ratio of irreversibility parameter Bejan number Be.

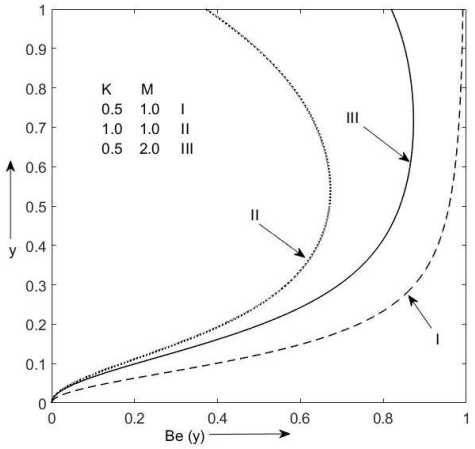

Fig. 15. Be profile versus y, when $h_1 = 1.0, P_2 = 1.0, Q = 1.0, K = 1.0, M = 2.0, P_1 = 1.0, Br = 0.5, Pr = 7.0$

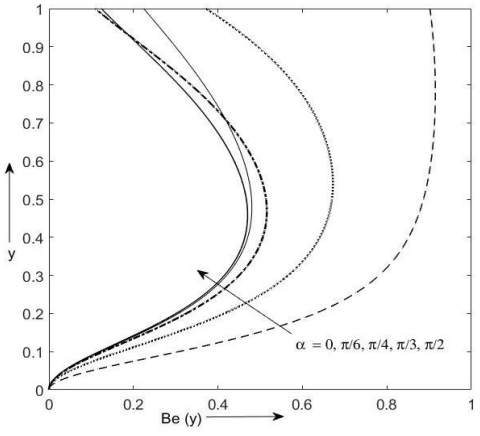

Fig. 15. Be profile versus y, when $h_1 = 1.0, P_2 = 1.0, Q = 1.0, K = 1.0, M = 2.0, P_1 = 1.0, Br = 0.5, Pr = 7.0$

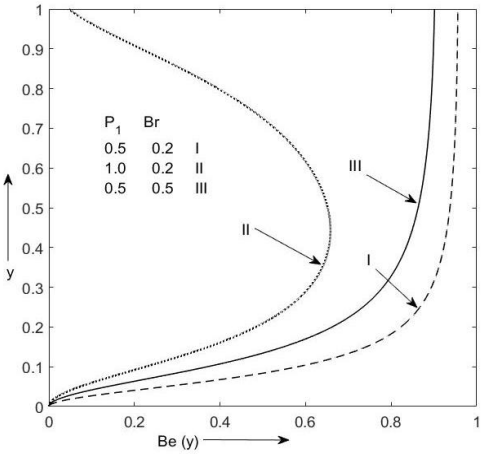

Fig. 16. Be profile versus y, when $h_1 = 1.0, P_2 = 1.0, Q = 1.0, \quad K = 1.0, M = 2.0, \alpha = \frac{\pi}{4}, Pr = 7.0$

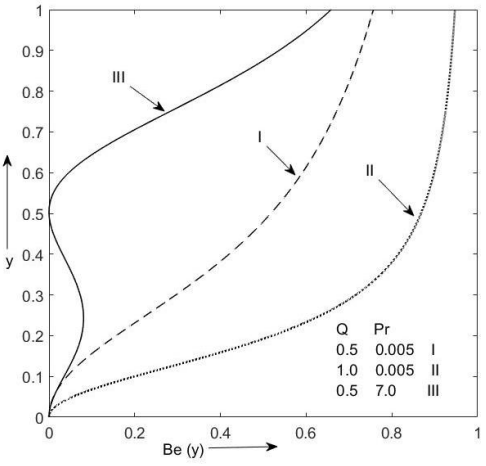

Fig. 17. Be profile versus y, when $h_1 = 1.0, P_2 = 1.0, P_1 = 1.0, K = 1.0, M = 2.0, \alpha = \frac{\pi}{4}, Br = 0.5$

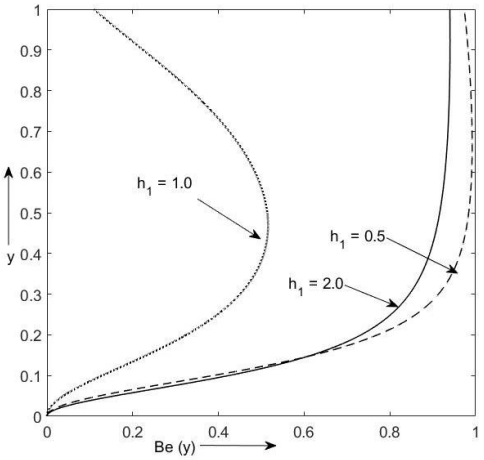

Fig. 18. Be profile versus y, when $Q_1 = 1.0, P_2 = 1.0, P_1 = 1.0\,, K = 1.0, \ M = 2.0, \alpha = \frac{\pi}{4}, \ Br = 0.5, Pr = 7.0.$

It is the valid reason for rising in the irreversibility parameter; because, the growth in the heat source Q boosts the fluid temperature and the total entropy generation, consequently the Bejan number Be increases. Similarly, a growth in the $\Pr$, from $\Pr = 0.005$ (liquid sodium) to $\Pr = 7.0$ (water) diminishes the irreversibility parameter ratio Bejan number Be. It is possible, because the rise in the Prandtl number declines the total entropy generation. Later, Fig. 18 explains the effect of the channel depth h_1 with Bejan number Be. This result shows that the irreversibility ratio Bejan number Be reduces with an increase in the depth of the channel from $h_1 = 0.5$ to $h_1 = 1.0$, but as the depth of the channel increases from $h_1 = 1.0$ to $h_1 = 2.0$, the Bejan number is enhanced and Bejan number achieves its maximum value 1 when the value of depth is taken $h_1 = 0.5$. The present analysis of Bejan number with the different physical parameters has been validated the typical range of Bejan number from 0 to 1 as discussed by Das et al. [31].

7.5. Skin friction coefficient and Nusselt number

Table 1 defines the numerical values of the coefficient of skin friction at the insulated bottom wall and upper surface of the channel. It is found that the coefficient of skin friction decreases at the bottom wall and upper surface of the channel; when the value of permeability, magnetic field, an inclination angle of magnetic field and Reynolds number increase, whereas, the growth in the strength of pressure gradient upsurges the coefficient of skin friction for the insulated bottom wall of the channel.

In the continuation, Table 2 defines the numerical values of the Nusselt number at the bottom wall and upper surface of the channel. It is found that the value of the Nusselt number increases at the bottom wall and upper surface of the channel when the strength of the pressure gradient, Prandtl number, Brinkmann number, and temperature gradient improve in the channel, whereas, an enhancement in the permeability, magnetic field, and inclination of magnetic field upsurges the Nusselt number at the bottom wall; while these flow parameters show the reverse effect at the upper surface of the channel.

Table 1. Numerical values of coefficient of skin friction at the insulated bottom wall and the upper open surface of the channel when $h_1 = 1.0$.

K	M	α	P_1	Re	$(C_{f_0})_{y=0}$	$(C_{f_1})_{y=h_1}$
0.5	1.0	$\pi/4$	0.5	1.0	0.8075	-1.1102× 10^{-16}
1.0	1.0	$\pi/4$	0.5	1.0	0.6867	-2.7756× 10^{-17}
0.5	**2.0**	$\pi/4$	0.5	1.0	0.7217	5.5511× 10^{-17}
0.5	1.0	$\boldsymbol{\pi/2}$	0.5	1.0	0.7217	0.0000
0.5	1.0	$\pi/4$	**1.0**	1.0	1.6151	-2.2204× 10^{-16}
0.5	1.0	$\pi/4$	0.5	**2.0**	0.2019	-2.7756× 10^{-17}

Table 2. Numerical values of Nusselt number at the insulated bottom wall and the upper open surface of the channel when $h_1 = 1.0$.

K	M	α	P_1	Q	Br	Pr	P_2	$(Nu)_{y=0}$	$(Nu)_{y=h_1}$
0.5	1.0	$\pi/4$	0.5	0.5	0.5	0.71	0.5	-3.2960× 10^{-17}	0.6850
1.0	1.0	$\pi/4$	0.5	0.5	0.5	0.71	0.5	0.0000	0.6077
0.5	**2.0**	$\pi/4$	0.5	0.5	0.5	0.71	0.5	0.0000	0.6218
0.5	1.0	$\boldsymbol{\pi/2}$	0.5	0.5	0.5	0.71	0.5	1.7347× 10^{-18}	0.6218
0.5	1.0	$\pi/4$	**1.0**	0.5	0.5	0.71	0.5	0.0000	0.9168
0.5	1.0	$\pi/4$	0.5	**1.0**	0.5	0.71	0.5	1.7347× 10^{-18}	1.6710
0.5	1.0	$\pi/4$	0.5	0.5	**0.7**	0.71	0.5	2.7756× 10^{-17}	0.7152
0.5	1.0	$\pi/4$	0.5	0.5	0.5	**7.0**	0.5	2.2204× 10^{-16}	0.7308
0.5	1.0	$\pi/4$	0.5	0.5	0.5	0.71	**1.0**	5.5511× 10^{-17}	0.6900

8. Conclusions

The main purpose of the present work is to analyze the irreversibility distributions in terms of entropy generation profile. Also, the irreversibility ratio is discussed in terms of Bejan number profile. In this analysis, we identify the physical parameters that help for optimizing the total irreversibility caused due to heat dissipation and magnetic field along with other physical parameters.

In the present analysis, we have some concluding remarks as:

I. Inclined magnetic field parameter M played a significant role in the present flow configuration. It is noticed that an improvement in the intensity of the inclined magnetic M develops the resistance in the fluid motion, and therefore the velocity and temperature of fluid decreases. Thus, the fluid motion and fluid temperature can be optimized with the appropriate change in the inclined magnetic field M .

II. The present study also predicts that the total irreversibility in the flow scheme can be controlled by changing the potential of magnetic field M and pressure gradient P_1.

III. The increment in the heat source Q boosts the fluid temperature, therefore the total entropy generation profile as well as and Bejan number profile rise.

IV. The rise in the inclination angle of magnetic field from $\alpha = 0$ to $\alpha = \pi/2$ helps to decrease the potential of fluid temperature and irreversibility parameter Ns, and as a result Bejan number Be also decreases.

This investigation will help the researchers for further study of the present fluid model with different boundary and geometrical conditions. Also, the present fluid model may discuss by using the different types of Newtonian and non-Newtonian fluid under the other atmospheric conditions. Such type of fluid flows are possible due to atmospheric pressure, therefore it has various applications in nature and industries; such as open river flow, streams, artificial channel flow, groundwater flow, irrigation ditches, and drains etc.

References

[1] A. A. Raptis, "Unsteady free convective flow through a porous medium", *International Journal of Engineering Science,* Vol. 21, No 4, pp. 345-348, (1983).

[2] S. P. Vanka and R. K. Ahluwalia, "Three-dimensional flow and thermal development in magnetohydrodynamic channels", *Journal of Energy,* Vol. 6, No. 3, pp. 218-224, (1982).

[3] S. K. Ghosh and P. K. Bhattacharjee, "Hall effects on steady hydromagnetic flow in a rotating channel in the presence of an inclined magnetic field", *Czechoslovak Journal of Physics,* Vol. 50, No. 6, pp. 759-767, (2010).

[4] D. V. Krishna, D. R. V. Prasad Rao and A. S. Ramachandra Murthy, "Hydromagnetic convection flows through a porous medium in a rotating channel", *Journal of Engineering Physics and Thermophysics*, Vol. 75, No. 2, pp. 281-291, (2002).

[5] A. K. Singh, "MHD free convective flow through a porous medium between two vertical parallel plates", *Indian Journal of Pure and Applied Physics,* Vol. 40, pp. 709-713, (2002).

[6] P. Y. Mhone and O. D. Makinde, "Unsteady MHD flow with heat transfer in a diverging channel", *Romanian Journal of Physics,* Vol. 51, No. 9, pp. 967-979, (2006).

[7] G. S. Seth, Raj Nandkeoylar, N. Mahto and S. K. Singh, "MHD couette flows in a rotating system in the presence of an inclined magnetic field", *Applied Mathematical Sciences,* Vol. 3, No. 59, pp. 2919-2932, (2009).

[8] G. S. Seth, Raj Nandkeolyar and Md. S. Ansari, "Hartmann flow in a rotating system in the presence of inclined magnetic field with hall effects", *Tamkang Journal of Science and Engineering,* Vol. 13, No. 3, pp. 243-252, (2010).

[9] W. A. Manyonge, D. W. Kiema and C.C.W. Lyaya, "Steady MHD Poiseuille

flow between two infinite parallel porous plates in an inclined magnetic field", *International Journal of Pure and Applied Mathematics,* Vol. 76, No. 5, pp. 661-668, (2012).

[10] K. M. Joseph, S. Daniel and G. M. Joseph, "Unsteady MHD couette flow between two infinite parallel porous plates in an inclined magnetic field with heat transfer", *International Journal of Mathematics and Statistics Invention,* Vol. 2, No. 3, pp. 103-110, (2014).

[11] K. V. S. Raju, T. S. Reddy, M. C. Raju, P. V. Satya Narayana and S. Venkataramana, "MHD convective flow through a porous medium in a horizontal channel with insulated and impermeable bottom wall in the presence of viscous dissipation and joule heating", *Ain Shams Engineering Journal,* Vol. 4, No. 2, pp. 543-551, (2014).

[12] A. Mburu and J. Kwanza, "Magnetohydrodynamic fluid flow between two parallel infinite plates subjected to an inclined magnetic field under pressure gradient", *Journal of Multidisciplinary Engineering Science and Technology (JMEST),* Vol. 3, No. 11, pp. 5910-5914, (2016).

[13] P. Sharma and R. Saboo, "A theoretical study of heat and mass transfer in forced convective chemically reacting radiating MHD flow though saturated porous medium over fixed horizontal channel", *AMSE-IIETA publication, Modelling, Measurement and Control C,* Vol. 78, No. 1, pp. 100-115, (2017).

[14] A. Bejan, "A study of entropy generation in fundamental convective heat transfer", *Journal of Heat Transfer,* Vol. 101, No. 4, pp. 718-725, (1979).

[15] A. Bejan, "Entropy generation minimization: the new thermodynamics of finite-size device and finite time processes", *Journal of Applied Physics,* Vol. 79, No. 3, pp. 1191-1218, (1996).

[16] S. Mahmud and R.A, Fraser, "Magnetohydrodynamic free convection and entropy generation in a square porous cavity", *International Journal of Heat and Mass Transfer,* Vol. 47, No. 14-17, pp. 3245-3256, (2004).

[17] S. Mahmud and R.A. Fraser, "Flow, thermal and entropy generation characteristics inside a porous channel with viscous dissipation", *International Journal of Thermal sciences,* Vol. 44, No. 1, pp. 21-32, (2005).

[18] R. A. Damesh, M. Q. Al-Odat and M.A. Al-Nimr, "Entropy generation during fluid flow in a channel under the effect of the transverse magnetic field", *Heat and Mass Transfer,* Vol. 44, No. 8, pp. 897-904, (2008).

[19] M. Bouabid, N. Hidouri, M. Magherbi and A.B. Brahim, "Analysis of the magnetic field effect on entropy generation at thermosolutal convection in a square cavity", *Entropy,* Vol. 13, No. 5, pp. 1034-1054, (2011).

[20] A. S. Eegunjobi and O.D. Makinde, "Effects of Navier slip on entropy generation in a porous channel with suction/injection" *Journal of Thermal Science and Technology*, Vol. 7, No. 4, pp. 522-535, (2012).

[21] A. S. Eegunjobi and O.D. Makinde, "Combined effect of buoyancy force and Navier slip on entropy generation in a vertical porous channel", *Entropy*, Vol. 14 No. 6, pp. 1028-1044, (2012).

[22] O. D. Makinde and A.S. Eegunjobi, "Analysis of inherent irreversibility in a variable viscosity MHD generalized Couette flow with permeable walls.", *Journal of Thermal Science and Technology*, Vol. 8, No. 1, pp. 240-254, (2013).

[23] Z. Mehrez, M. Bouterra, A.E. Cafsi and A. Belghith, "Heat transfer and entropy generation analysis of nanofluids flow in an open cavity", *Computers and Fluids,* Vol. 88, pp. 363-373, (2013).

[24] S. O. Adesanya and O.D. Makinde, "Entropy generation in couple stress fluid flow through porous channel with fluid slippage", *International Journal of Exergy,* Vol. 15, No. 3, pp. 344-362. (2014).

[25] S. O. Adesanya and O.D. Makinde, "Effects of couple stresses on entropy generation rate in a porous channel with convective heating", *Computational and Applied Mathematics*, Vol. *34, No.* 1, pp. 293-307, (2015).

[26] O. D. Makinde and A.S. Eegunjobi, "Entropy analysis of thermally radiating magnetohydrodynamic slip flow of Casson fluid in a microchannel filled with saturated porous media*", Journal of Porous Media*, Vol. 19, No. 9, pp.799-810, (2016).

[27] P. Sharma, T. Sharma and N. Kumar, "Entropy analysis in MHD forced convective flow through a circular channel filled with the porous medium in the presence of thermal radiation", *International Journal of HeatTechnology*, Vol. 34, No. 2, pp. 311-318, (2016).

[28] K. Yamamoto and N. Iwamura, "Flow with convective acceleration through a porous medium", *Journal of Engineering Mathematics*, Vol. 10, No. 1, pp. 41-54, (1976).

[29] L. C. Woods, "The thermodynamics of fluid systems", Oxford *Engineering Science Series, Clarendon press* (1975).

[30] A. Bejan, "Entropy generation through heat and fluid flow", *Wiley*, (1982).

[31] S. Das and R.N. Jana, "Entropy generation due to MHD flow in a porous channel with navier slip", *Ain Shams Engineering Journal*, Vol. 5, No. 2, pp. 575-584, (2014).

How to cite this paper:

Tarun Sharmaa, Pooja Sharmab, and Navin Kumar, *"* Entropy generation analysis of MHD forced convective flow through a horizontal porous channel*", Journal of Computational and Applied Research in Mechanical Engineering*, Vol. 10, No. 1, pp. 37-49, (2020).

DOI: 10.22061/jcarme.2019.5039.1615

URL: http://jcarme.sru.ac.ir/?_action=showPDF&article=1118